NREL
NATIONAL RENEWABLE ENERGY LABORATORY

An Integrated Approach Using Condition Monitoring and Modeling to Investigate Wind Turbine Gearbox Design

Preprint

S. Sheng and Y. Guo
National Renewable Energy Laboratory

To be presented at ASME Turbo Expo 2015: Turbine Technical Conference and Exposition
Montréal, Canada
June 15–19, 2015

NREL is a national laboratory of the U.S. Department of Energy
Office of Energy Efficiency & Renewable Energy
Operated by the Alliance for Sustainable Energy, LLC

This report is available at no cost from the National Renewable Energy Laboratory (NREL) at www.nrel.gov/publications.

Conference Paper
NREL/CP-5000-60978
March 2015

Contract No. DE-AC36-08GO28308

NOTICE

This report is available at no cost from the National Renewable Energy Laboratory (NREL) at www.nrel.gov/publications.

Available electronically at http://www.osti.gov/scitech

Available for a processing fee to U.S. Department of Energy and its contractors, in paper, from:

U.S. Department of Energy
Office of Scientific and Technical Information
P.O. Box 62
Oak Ridge, TN 37831-0062
phone: 865.576.8401
fax: 865.576.5728
email: mailto:reports@adonis.osti.gov

Available for sale to the public, in paper, from:

U.S. Department of Commerce
National Technical Information Service
5285 Port Royal Road
Springfield, VA 22161
phone: 800.553.6847
fax: 703.605.6900
email: orders@ntis.fedworld.gov
online ordering: http://www.ntis.gov/help/ordermethods.aspx

Cover Photos: (left to right) photo by Pat Corkery, NREL 16416, photo from SunEdison, NREL 17423, photo by Pat Corkery, NREL 16560, photo by Dennis Schroeder, NREL 17613, photo by Dean Armstrong, NREL 17436, photo by Pat Corkery, NREL 17721.

AN INTEGRATED APPROACH USING CONDITION MONITORING AND MODELING TO INVESTIGATE WIND TURBINE GEARBOX DESIGN

Shuangwen Sheng
National Renewable Energy Laboratory
Golden, Colorado, USA
shuangwen.sheng@nrel.gov

Yi Guo
National Renewable Energy Laboratory
Golden, Colorado, USA
yi.guo@nrel.gov

ABSTRACT

Vibration-based condition monitoring (CM) of geared utility-scale turbine drivetrains has been used by the wind industry to help improve operation and maintenance (O&M) practices, increase turbine availability, and reduce O&M cost. This study is a new endeavor that integrates the vibration-based CM technique with wind turbine gearbox modeling to investigate various gearbox design options. A team of researchers performed vibration-based CM measurements on a damaged wind turbine gearbox with a classic configuration, (i.e., one planetary stage and two parallel stages). We observed that the acceleration amplitudes around the first-order sidebands of the intermediate stage gear set meshing frequency were much lower than that measured at the high-speed gear set, and similar difference was also observed in a healthy gearbox. One factor for a reduction at the intermediate stage gear set is hypothesized to be the soft sun-spline configuration in the test gearbox. To evaluate this hypothesis, a multibody dynamic model of the healthy test gearbox was first developed and validated. Relative percent difference of the first-order sidebands—of the high-speed and intermediate stage gear-meshing frequencies—in the soft and the rigid sun spline configurations were compared. The results verified that the soft sun-spline configuration can reduce the sidebands of the intermediate stage gear set and also the locating bearing loads. The study demonstrates that combining vibration-based CM with appropriate modeling can provide insights for evaluating different wind turbine gearbox design options.

KEYWORDS

Wind turbine, condition monitoring, gearbox modeling, design, analysis

NOMENCLATURE

c	=	contact ratio
d	=	distance
k	=	stiffness
k_m	=	normal stiffness
t	=	time

1. INTRODUCTION

Wind energy is one of the fastest growing renewable energy sources in the world. However, the industry still experiences premature turbine component failures leading to increased cost of energy (COE). To make wind energy more competitive, there is a need for the industry to increase component reliability and turbine availability. Among the various subsystems comprising a geared utility-scale wind turbine, the gearbox has been shown to cause the most downtime and is also the most costly to maintain throughout a turbine's 20-year design life [1]. To understand the causes of premature failures in wind turbine gearboxes and propose possible improvements to the wind industry, the National Renewable Energy Laboratory (NREL) formed a consortium called the Gearbox Reliability Collaborative (GRC) [2]. The GRC brings together different parties involved in gearbox design, manufacture, and maintenance with the goal of improving gearbox reliability and increasing turbine availability. Condition monitoring (CM) was started as one research area under the GRC. Its main benefit is to help the industry improve operation and maintenance (O&M) practices, increasing turbine availability and reducing the COE. This study, however, is a new endeavor toward integrating vibration-based CM with wind turbine gearbox modeling to investigate different gearbox design options. It demonstrates additional benefits that can be gained in addition to the immediate improvements in turbine availability from wind turbine

drivetrain CM. Normally, high-frequency dynamic responses of turbine drivetrain components in a utility-scale wind turbine—in the several-kilohertz range—cannot be obtained by the turbine supervisory control and data acquisition (SCADA) system unless the turbine is equipped with a vibration-based CM system. One potential application area of the proposed approach is a design improvement of already widely deployed commercial turbines or their subsystems based on testing. The uniqueness of this design evaluation is its backward approach, which begins with observations made through vibration-based CM systems.

Under the GRC, two 750-kW test gearboxes with a classic configuration of one planetary stage and two parallel stages were examined. One of the two test gearboxes was sent to a wind plant near NREL for a field test after its run-in. During the field test, it experienced two oil-loss events leading to damage to its internal gears and bearings. The test gearbox was then removed from the field and retested at NREL's 2.5-MW dynamometer test facility [3], where vibration-based CM measurements were taken. It was observed that the acceleration amplitude of the first-order sidebands around the intermediate stage gear set meshing frequency was much lower than that measured at the high speed stage gear set [4]. Because damage occurred at the high-speed and intermediate-speed stages were both classified as severe in the failure analysis, it is reasonable to assume that the amplitude difference in the first-order sidebands of these two gear sets is not likely caused only by the variation in damage levels [5]. Further evaluation based on a healthy gearbox revealed similar difference between the first-order sidebands at the intermediate and high-speed stage gear sets. As a result, the low amplitude of sidebands at the intermediate stage gear set may also be related to the gearbox design. One factor we hypothesized was the floating sun configuration, which is supposed to reduce the effects of bending loads from the planetary stage to the two parallel stages. To evaluate this hypothesis, a multibody dynamic model of the healthy test gearbox was developed in SIMPACK [6]. After validating the model, we compared the relative percent difference of the first-order sidebands of the high- and intermediate-shaft gear-meshing frequencies between the soft and the rigid sun spline configurations.

The rest of the paper is organized as follows. First, a brief discussion of the test gearbox, test conditions, and damage is provided. Then, the observations obtained through the vibration-based CM systems are presented. Next, the modeling of the test gearbox is introduced and its validation follows. The gearbox dynamic responses under different design options are then simulated and evaluated. Finally, this paper concludes with some discussion and future work.

2. TEST GEARBOX, EXPERIMENT DESCRIPTION, AND DAMAGED GEARS

The GRC test gearbox is designed for a stall-controlled, three-bladed, upwind turbine, with a rated power of 750 kW. The turbine generator operates at either 1800 rpm or 1200 rpm, depending on the wind conditions. The gearbox has an overall ratio of 1:81.49. It is composed of one low-speed planetary stage and two parallel stages, as shown in Figure 1. Nomenclature for its internal elements is described in Figure 2, and the number of gear teeth for each gear and the gear ratios are listed in Table 1. Several types of bearings [7] are employed in the test gearbox, according to the loading conditions and gearbox life requirements. The planet carrier (PLC) is supported by two full-complement cylindrical roller bearings (CRBs). Each planet gear is supported by two identical CRBs. Each parallel shaft (i.e., low, intermediate, and high speed) in the gearbox is supported by a CRB on the upwind (rotor) side, and by two back-to-back mounted, tapered roller bearings (TRBs) on the downwind (generator) side. The gearbox first finished its run-in in the NREL 2.5-MW dynamometer test facility [3] and was later sent to a wind plant near NREL for field tests, where two oil-loss events occurred. Further field operation of the test gearbox was terminated to avoid the possibility of a catastrophic failure.

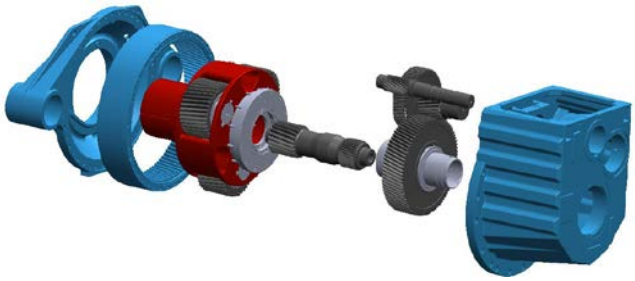

Figure 1. Test gearbox exploded view.

The test gearbox was removed from the field and retested in the NREL dynamometer test facility. During the dynamometer retest, various vibration-based CM systems were employed [8]. The locations of two accelerometers investigated in this study—AN6 and AN7—are shown in Figure 3. Sensor AN6 is mainly used to monitor the radial vibration of gears and bearings on the intermediate-speed shaft (IMS), including both intermediate- and high-speed stages. Sensor AN7 is mainly used to monitor the radial vibration of gears and bearings on the high-speed shaft (HSS), i.e. high-speed stage. The vibration data collected under three testing conditions, as illustrated in Table 2, are used in this study. Figure 4 is a photo of the dynamometer retest implementation with the test gearbox installed.

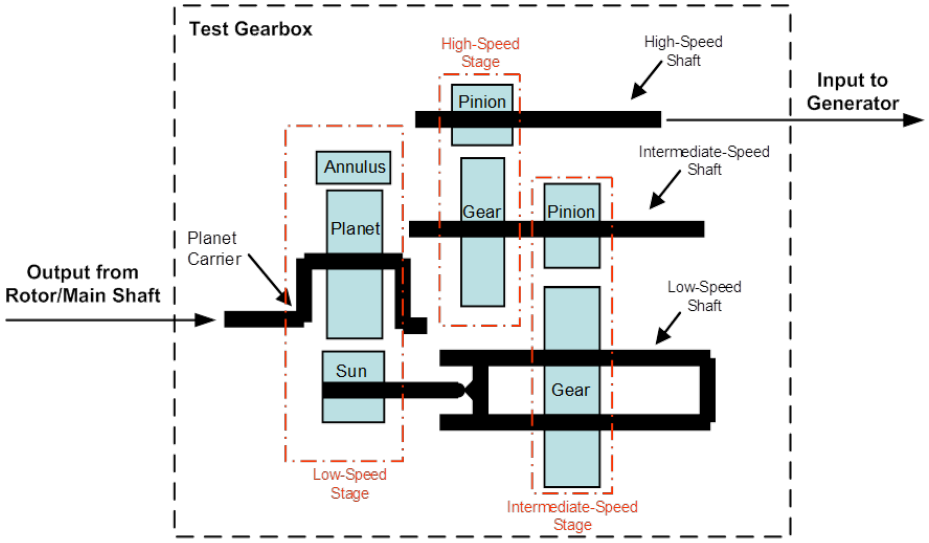

Figure 2. Test gearbox internal nomenclature and abbreviations.

Table 1. Gear-teeth number and ratio.

Gear Element	No. of Teeth	Mate Teeth	Ratio
Ring gear	99	39	
Planet gear	39	99	
Sun pinion	21	39	5.71
Intermediate pinion	23	82	3.57
High-speed shaft gear	88	22	
High-speed shaft pinion	22	88	4.00
Total gear ratio			81.49

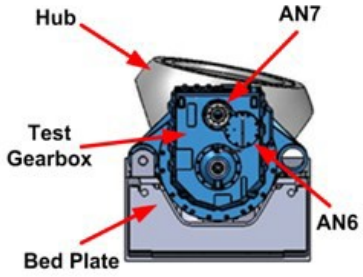

Figure 3. Location of accelerometers AN6 and AN7.

Table 2. Gearbox test conditions.

Test Case	Nominal HSS Speed (rpm)	Input Shaft Torque (% of rated torque)
2a	1,200	25%
2b	1,800	25%
2c	1,800	50%

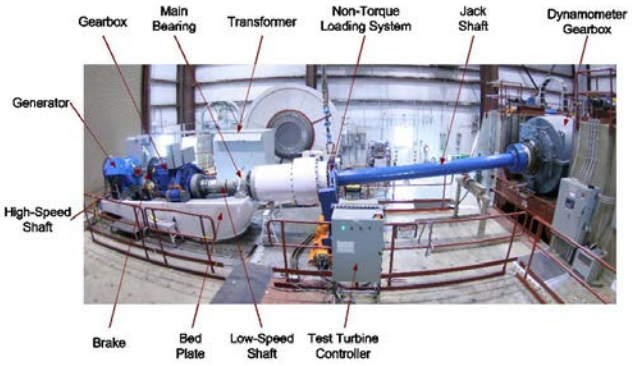

Figure 4. NREL dynamometer test stand with the test article installed. Photo by Lee Jay Fingersh, NREL 16913.

After the dynamometer retest, the gearbox was sent to a rebuild shop, where it was disassembled and a detailed failure analysis [5] was conducted. The damage observed on the HSS gear set was severe scuffing. The IMS gear set also had scuffing and fretting corrosion on the teeth. The level of damage for both stages was determined to be severe [5]. Photos of the damage tothe HSS and IMS gear set teeth are provided in Figures 5 and 6, respectively. The root cause of the faults was oil starvation resulting from the two oil-loss events during the field test.

Figure 5. HSS gear set damage. Photo from GEARTECH, NREL 19599.

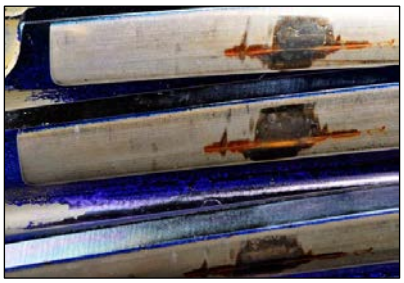

Figure 6. IMS gear set damage. Photo from GEARTECH, NREL 19745.

3. OBSERVATIONS BY VIBRATION-BASED CM SYSTEMS

During the dynamometer retest of the damaged gearbox, acceleration data were collected by various CM systems [7,8]. Each test condition listed in Table 2 was run for about 10 minutes. Based on the torque and HSS rotational speed measurements, obtained under test case 2c by the NREL-customized vibration-based CM system [9], it was determined that 8 out of the 10 minutes of data were representative. A spectrum analysis was conducted on the eight minutes of data collected by sensors AN6 and AN7 at eight discrete instances and eight spectra were generated for each accelerometer. To evaluate the damage that occurred to the test gearbox, a condition indicator, referred to as sideband index (SI) and calculated according to Equation (1) [4,10], was used, where *sb* stands for sideband, *R* represents regular meshing components, *GMF* is gear meshing frequency of the interested gear pair, and -1 and +1 indicate the first-order sidebands.

$$SI = (R^{sb}_{GMF,-1}(x) + R^{sb}_{GMF,+1}(x))/2 \quad (1)$$

Because of the minor speed variances during testing [9] and the lack of a one-pulse-per-shaft-revolution signal, the values of $R^{sb}_{GMF,-1}(x)$ and $R^{sb}_{GMF,+1}(x)$ were determined by increasing the frequency range to above and below each sideband by 2.5 Hz. For example, for the left first-order sideband of HSS GMF, under a high speed shaft rotational speed of 30 Hz, the value of *(x)* at sideband 630 Hz was determined to be the sum of spectrum $R^{sb}_{GMF,-1}$ values between 627.5 Hz and 632.5 Hz.

Figure 7 shows the SI values (Unit: g) calculated based on vibration data collected during test case 2c from the damaged test gearbox by accelerometers AN6 and AN7 for the HSS and IMS gear sets. The figure clearly shows that SI values from the HSS gear set are much higher than those from the IMS gear set. Such a big difference may not be caused by damage to the gear sets alone, because they were both classified as severe. It might be related to the test gearbox configuration.

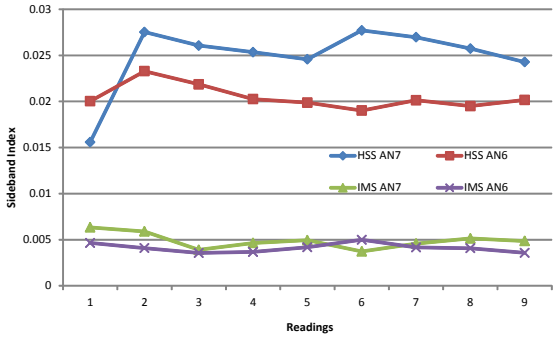

Figure 7. Sideband index from AN6 and AN7 for the damaged gearbox.

To investigate whether the difference is related to the test gearbox configuration, vibration data was collected by sensors that were mounted at locations equivalent to AN6 and AN7 when the test gearbox was being run-in and considered "healthy" under testing condition case 2c at the NREL dynamometer test facility. Figure 8 shows the SI values for these two gear sets collected by the two sensors. The figure also shows that the SI values from the HSS gear set are higher than those from the IMS gear set; however, the difference is not as dramatic as in the damaged test gearbox case. In addition, it appears that the HSS gear set SI values measured by AN6 are very high, which might be caused by an axial offset made to the high-speed gear set for assembly reasons and the heavy driving gear weight of the HSS gear set located on the intermediate-speed shaft.

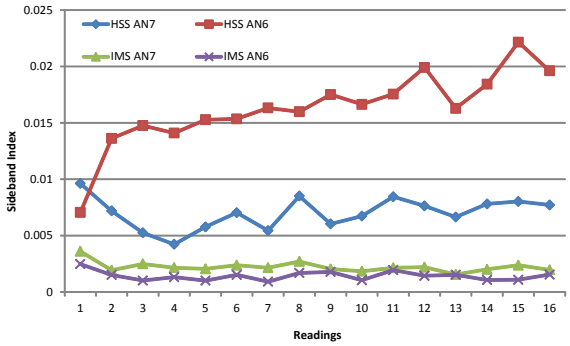

Figure 8. Sideband index from AN6 and AN7 for the healthy gearbox.

When comparing the SI values shown in Figures 7 and 8, it is reasonable to conclude that the SI values are not only a function of gear set damage but are affected by the gearbox configuration. One possible factor leading to such a big difference between the two gear sets is the floating sun spline configuration of the test gearbox, but evaluation requires that a comparison be made against a fixed sun spline configuration. Ideally, such an evaluation would require data collection under the same test conditions from another gearbox, with everything being the same as the gearbox investigated in this study except that the sun spline is fixed; however, this is not feasible. With advances in modeling capabilities of wind turbine drivetrains [11], a modeling approach to compare the floating and fixed sun spline configurations is proposed in this study and discussed in the following sections. It should be noted that the fixed and floating sun spline configurations are only compared in an approximate sense by increasing the tilting stiffness of the sun spline to simulate the fixed configuration, rigid sun spline, and reducing it to simulate the floating configuration, soft sun spline.

4. DYNAMIC MODELING OF THE TEST GEARBOX

A three-dimensional multibody dynamic model of the test gearbox was established in SIMPACK [6]. The model includes an input shaft to the gearbox as shown in Figure 9. Generator coupling (not shown) is modeled by its stiffnesses specified by the coupling manufacturer.

Gears are modeled by rigid bodies with six degrees of freedom. The gear-contact analysis considers the time-varying tooth meshing that is the fundamental excitation source inside the gearbox according to ISO 6336 [12]. To consider gear-tooth microgeometries and profile/crown modifications that affect gear dynamics, each gear element is divided into many slices. Thirty-five tooth slices are selected in this research based on a convergence study [13]. An illustration of the gear-tooth load distribution at the sun-planet mesh is shown in Figure 10.

Bearings are modeled using their stiffness matrices with bearing clearance nonlinearities. The clearances can help bearings accommodate thermal expansion, interference fit, and surface roughness. However, they can also cause gear-tooth misalignment that leads to uneven tooth and bearing load distribution and elevated vibration [14,15]—in particular, with the presence of nontorque loads in wind turbines. The equivalent stiffness with bearing clearance is an order of magnitude smaller than that without clearance under the operating loading condition.

This model also includes the flexibilities of important structural components, such as the input shaft, planet carrier, parallel stage shafts, and gearbox housing. Integrating the flexible housing and carrier into the gearbox model consists of two steps: 1) establishing a finite-element mesh of these components, and 2) integrating their finite-element meshes into the gearbox model through dynamic modal condensation [16]. Shafts are modeled using beam elements.

An articulated sun spline connection between the planetary gear stage and the IMS stage, often adopted to float the sun in wind turbine gearboxes, is used in the GRC gearbox and allows a certain amount of radial and tilting motions of the sun gear. The spline is modeled by its diagonal stiffness matrix obtained from the finite-element analysis using the RomaxWIND [17] spline model. The spline stiffnesses are illustrated in Table 3. The tilting stiffness of the spline is used to simulate whether the sun is floating. For the GRC test gearbox, the nominal spline tilting stiffness equals 3.5×10^6 Nm/rad. This study investigates the vibration responses at the IMS and HSS gear sets by reducing the sun spline stiffness from its nominal to simulate the floating, or soft sun spline, and by increasing it from the nominal to simulate the fixed, or rigid sun-spline, configurations. For rigid sun spline, a stiffness value of 10×10^9 Nm/rad was used and for soft sun spline, it was reduced to 3.5×10^3 Nm/rad (three orders of magnitude smaller than the nominal tilting stiffness). The applied torque and load used in this model were defined based on the measurement data collected from the dynamometer test of the gearbox.

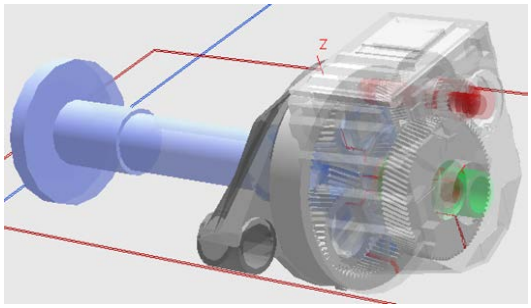

Figure 9. Multibody dynamic model of the GRC gearbox established in SIMPACK.

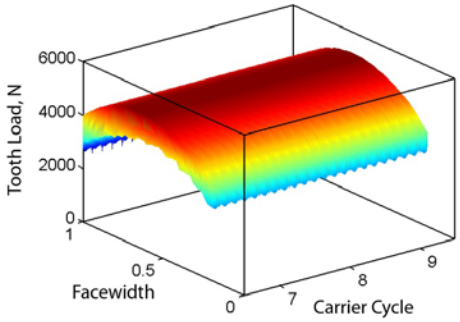

Figure 10. Gear-tooth load distribution at the sun-planet mesh.

Table 3. Sun-spline stiffnesses.

Radial Stiffness (N/m)	Axial Stiffness (N/m)	Tilting Stiffness (Nm/rad)	Rotational Stiffness (Nm/rad)
20×10^9	0	$3.5 \times 10^3, 10 \times 10^9$	10×10^9

5. MODEL VALIDATION FOR VIBRATION ANALYSIS

The model has been validated against GRC experiments for gear and bearing loads in the planetary stage [13,16]. Those validations focused on the mean and peak-to-peak loads in the time domain and have not studied gearbox vibrations. Additional model validation of gearbox displacements and accelerations in both the time and frequency domains is crucial for vibration analyses. The vibration-based CM systems use a set of accelerometers with high bandwidth, which can measure gearbox vibrations up to several kilohertz. These vibration signals can help characterize broad vibration spectra of wind turbine gearboxes—up to three or more harmonics of the HSS mesh frequencies. The CM system provides important experimental data that benchmark the developed model for vibration analysis.

Figure 11 compares the sun-gear orbiting time history at rated torque (325 kNm) between the model with a nominal sun spline tilting stiffness and the GRC experiments with a main-shaft pitching moment of 95 kNm. Excellent agreement between the model and experimental results demonstrates that the model is capable of capturing the sun orbiting trajectories, which also indicates that the sun spline is modeled accurately. Spectra of simulated vibration under the test case 2c, measured by radial displacements, for the IMS and HSS stages are shown in Figure 12 and Figure 13, respectively. The experimental data are measured at accelerometers AN7 on the HSS and AN6 on the IMS. Good agreement between the model and experiment is evident on mesh-frequency harmonics, including harmonics of planetary-gear mesh frequency ω_m^{PG}, intermediate-stage mesh frequency ω_m^{IM}, and high-speed-stage mesh frequency ω_m^{HS}, with frequency modulations from IMS and HSS rotation frequencies ω_s^{IM} and ω_s^{HS}. The experimental spectra at ω_m^{PG} and its harmonics are higher than the modeling results because the planetary ring gear with micropitting damage was reused during this dynamometer test, but the ring gear was considered healthy in the model. The modeling results match the experiments reasonably well considering the rich excitation sources in the test gearbox during the tests.

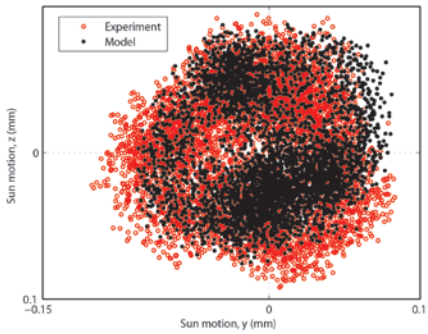

Figure 11. Comparison of the sun-gear orbiting motion between the developed model and the GRC experiments.

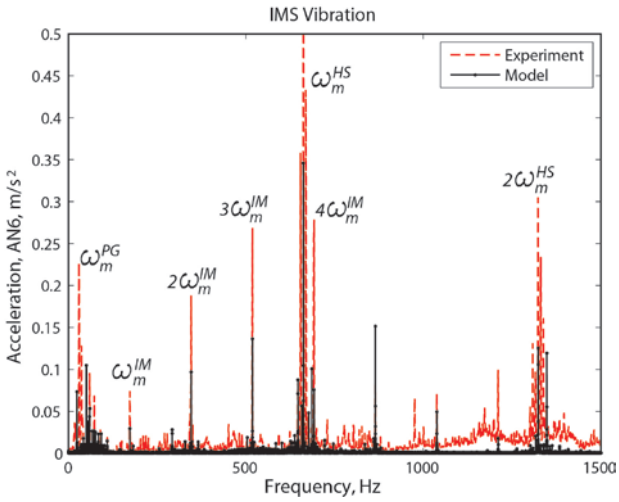

Figure 12. Spectra of the IMS radial acceleration of the tested healthy gearbox under test case 2c.

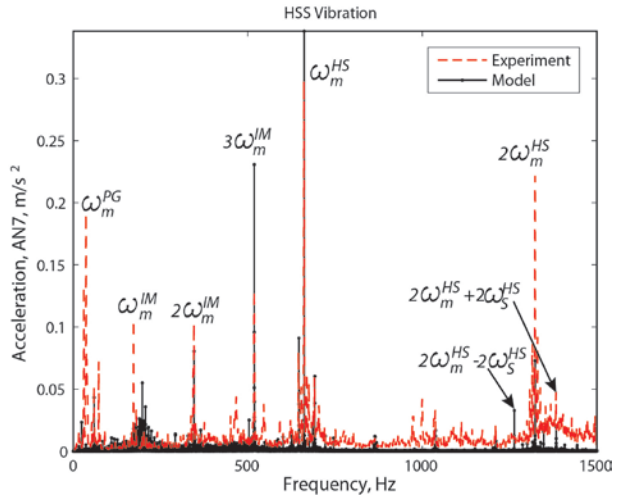

Figure 13. Spectra of the HSS radial acceleration of the tested healthy gearbox under test case 2c.

6. MODELING RESULTS AND DISCUSSIONS

Use of articulated sun spline in a wind turbine gearbox improves planetary load sharing by allowing sufficient self-adjusting orbiting motion of the sun gear; however, discussion of the influences of sun spline on vibration signatures of IMS and HSS gear sets are limited in the literature. This investigation was motivated by the observed difference between the first-order sidebands of the IMS and the HSS gear sets in both the healthy and damaged test gearboxes. Based on the validated model, two design options were examined: 1) soft sun spline to simulate the floating option, and 2) rigid connection between the sun shaft and the hollow shaft, mimicking the nonfloating option.

Figures 14 and 15 show the vibration spectra of IMS and HSS, respectively, at AN6 and AN7 locations with soft (option 1) and rigid (option 2) sun splines under rated torque with main-shaft pitching moment of 95 kNm. With soft sun spline,

the spectra have more frequency components and elevated amplitudes than the rigid connection design, particularly at the IMS stage. To quantitatively examine the impacts of sun-spline configuration, the SI values of the IMS gear set and HSS gear set in both rigid and soft sun-spline configurations were calculated using Equation (1), without the frequency range increase around the sidebands, as only a clean 30-Hz HSS rotational speed was simulated, based on the results shown in Figures 14 and 15.

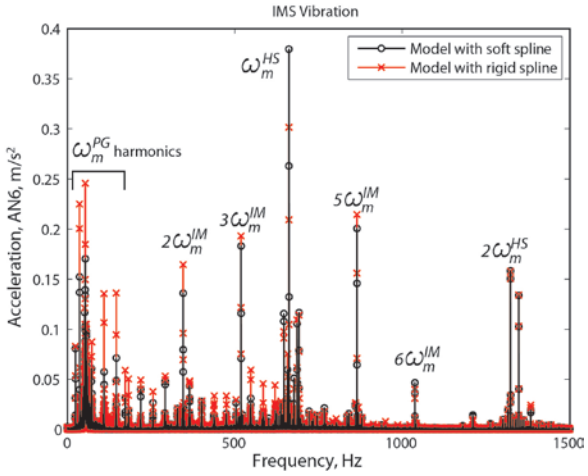

Figure 14. Spectra of the IMS radial acceleration with soft sun spline and rigid sun spline.

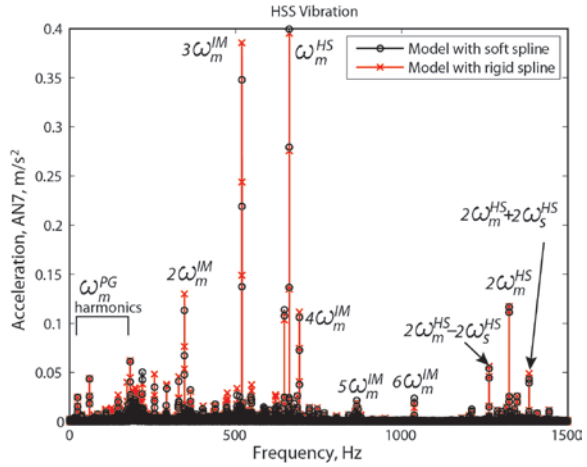

Figure 15. Spectra of the HSS radial acceleration with soft sun spline and rigid sun spline.

Table 4. Modeled SI values relative reduction.

Gear Set	Sun Spline	SI Values (m/s^2)	Percent Difference (%)
IMS	Rigid	0.00733	61.3
	Soft	0.00284	
HSS	Rigid	0.06209	0.1
	Soft	0.06205	

The values of $R^{sb}_{GMF,-1}(x)$ and $R^{sb}_{GMF,+1}(x)$ were determined by averaging readings of first-order sidebands in Figures 14 and 15. As shown in Table 4, soft sun spline configuration has a huge impact on the SI values of the IMS gear set and led to about 61.3% reduction as compared with rigid sun spline configuration, but does not have much impact on the SI values of the HSS gear set. The results demonstrated that the soft sun spline design can reduce sidebands or modulation level at the IMS gear set.

To further study the benefits of soft sun spline design, the downwind-side tapered roller bearing (denoted as TRB C) loads on the low-speed shaft (LSS), IMS, and HSS under the same loading conditions as Figures 14 and 15 were examined and are plotted in Figure 16. The soft sun spline design option can reduce the bearing loads from 6.0% to 14.3%, leading to improved bearing lives. It demonstrates that soft sun spline design reduces bearing loads on the LSS, IMS and HSS, especially to the LSS stage.

In summary, the soft sun spline configuration is advantageous in terms of: 1) reducing sidebands at the IMS stage, and 2) reducing locating bearing loads and helping improve bearing lives.

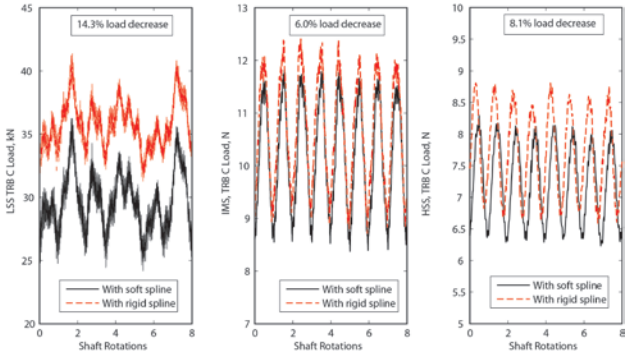

Figure 16. Bearing loads of the downwind-side TRB on the LSS, IMS, and HSS.

7. CONCLUSIONS

This paper has presented an approach that integrates vibration-based CM system responses with wind turbine gearbox modeling to evaluate various gearbox design options. This approach is motivated by some nonintuitive observations obtained by the vibration-based CM systems. The developed gearbox dynamic model has been validated against experimental data measured by the CM systems in both time and frequency domains. Good agreement between the model-predicted vibration spectra and experimental data is evident for the healthy test gearbox. Based on the validated model, we studied two design options, i.e., with a soft or a rigid sun spline. The results demonstrated that using a soft sun spline connection between the sun gear and the LSS reduces

sidebands of IMS gear set and locating bearing loads on all stages, resulting in improved gear and bearing lives.

The study illustrated that the proposed approach can provide insight into wind turbine gearbox dynamic responses under different design changes. In a commercial utility-scale wind turbine without a vibration-based CM system, high-frequency responses from gearboxes are not typically measured. This research has demonstrated that some additional benefits for turbine component design can be attained by wind turbine CM, in addition to its main contribution to help improve wind turbine and plant O&M practices. Furthermore, the proposed approach has the general advantage of cost saving obtained by modeling rather than conducting experiments. For future work, a model with a better representation of the fixed sun spline configuration will be developed and corresponding vibration analysis at the IMS and HSS stages will be conducted. Other gearbox design options and their impacts on gear set vibration, such as the hunting gear ratio of the HSS gear set, will be investigated. The model can be further developed to incorporate certain gearbox component failure mode.

ACKNOWLEDGMENTS

This work was supported by the U.S. Department of Energy under Contract No. DE-AC36-08GO28308 with the National Renewable Energy Laboratory. Funding for the work was provided by the DOE Office of Energy Efficiency and Renewable Energy, Wind and Water Power Technologies Office. The authors thank Yihan Xing from the Norwegian University of Science and Technology for valuable discussions on the model developed in this work. Additionally, we acknowledge and appreciate the support provided by the NREL Gearbox Reliability Collaborative team and project partners.

REFERENCES

[1] Link, H., LaCava, W., van Dam, J., McNiff, B., Sheng, S., Wallen, R., McDade, M., Lambert, S., Butterfield, S., and Oyague, F., "Gearbox Reliability Collaborative Project Report: Findings from Phase 1 and Phase 2 Testing," NREL/TP-5000-51885, 2011.

[2] Sheng, S., and Veers, P., "Wind Turbine Drivetrain Condition Monitoring—An Overview," Proceedings of the Machinery Failure Prevention Technology (MFPT): The Applied Systems Health Management Conference, Dayton, OH, 2011.

[3] National Renewable Energy Laboratory, "Dynamometer Testing (Fact Sheet)," NREL/FS-5000-45649, 2011.

[4] Dempsey P., and Sheng, S., "Investigation of Data Fusion for Health Monitoring of Wind Turbine Drivetrain Components," Wind Energy (to be published).

[5] Errichello, R., and Muller, J., "Gearbox Reliability Collaborative Gearbox 1 Failure Analysis Report," NREL/SR-5000-530262, 2012.

[6] SIMPACK, Multi-Body Simulation Software, Software Package, Ver. 8.904, Gilching Germany, 2011.

[7] Sheng, S., Link, L., LaCava, W., van Dam, J., McNiff, B., Veers, P., Keller, J., Butterfield, S., and Oyague, F., "Wind Turbine Drivetrain Condition Monitoring During GRC Phase 1 and Phase 2 Testing," NREL/TP-5000-52748, 2011.

[8] Sheng, S., "Investigation of Various Condition Monitoring Techniques Based on a Damaged Wind Turbine Gearbox," Proceedings of the 8th International Workshop on Structural Health Monitoring Conference, Stanford, CA, 2011.

[9] Sheng, S., "Wind Turbine Gearbox Condition Monitoring Round Robin Study – Vibration Analysis," NREL/TP-5000-54530, 2012.

[10] Antolick, L.J., Branning, J.S., Wade, D.R., and Dempsey, P.J., "Evaluation of Gear Condition Indicator Performance on Rotorcraft Fleet," Proceedings of the American Helicopter Society 66th Annual Forum, 2010.

[11] Peeters, J., Vandepitte, D., and Sas, P., "Structural Analysis of a Wind Turbine and Its Drive Train Using the Flexible Multibody Simulation Technique," Proceedings of the International Conference on Noise and Vibration Engineering, 2006.

[12] American Gear Manufacturers Association, "ISO 6336: Calculation of Load Capacity of Spur and Helical Gears," 2006.

[13] LaCava, W., Xing, Y., Guo, Y., and Torgeir, M., "Determining Wind Turbine Gearbox Model Complexity Using Measurement Validation and Cost Comparison," Proceedings of European Wind Energy Association Annual Event (to be published), Copenhagen, Denmark, 2012.

[14] Guo, Y., and Parker, R. G., "Dynamic Modeling and Analysis of a Spur Planetary Gear Involving Tooth Wedging and Bearing Clearance Nonlinearity," European Journal of Mechanics A/Solids, Vol. 29, No. 6, Nov.–Dec. 2010, pp. 1022–1033.

[15] Crowther, A., Ramakrishnan, V., Zaidi, N.A., and Halse, C., "Sources of Time-Varying Contact Stress and Misalignments in Wind Turbine Planetary Sets," Wind Energy, Vol. 14, No. 5, 2011, pp. 637–651.

[16] Guo, Y., Keller, J., and LaCava, W., "Combined Effects of Input Torque, Non-Torque Load, Gravity, and Bearing Clearance on Planetary Gear Load Share in Wind Turbine Drivetrains," AGMA Fall Technical Meeting, 2012.

[17] RomaxWIND, A Virtual Product Development and Simulation Environment for the Design and Analysis of Wind Turbine Gearboxes, Bearings and Drivetrains, Software Package, Ver. R14.0, Nottingham, England, 2011.